Overexpression of Elafin in Ovarian Carcinoma Is Driven by Genomic Gains and Activation of the Nuclear Factor κB Pathway and Is Associated with Poor Overall Survival[1,2]

Adam Clauss[*,†,3], Vivian Ng[*,3], Joyce Liu[*,†], Huiying Piao[*], Moises Russo[*,†], Natalie Vena[‡], Qing Sheng[†,§], Michelle S. Hirsch[†,¶], Tomas Bonome[#], Ursula Matulonis[*,†], Azra H. Ligon[†,‡,¶], Michael J. Birrer[†,**] and Ronny Drapkin[*,†,‡,¶]

*Dana-Farber Cancer Institute, Department of Medical Oncology, Boston, MA, USA; †Harvard Medical School, Boston, MA, USA; ‡Dana-Farber Cancer Institute, Center for Molecular Oncologic Pathology, Boston, MA, USA; §Dana-Farber Cancer Institute, Department of Cancer Biology, Boston, MA, USA; ¶Brigham and Women's Hospital, Department of Pathology, Boston, MA, USA; #National Institutes of Health, Molecular Mechanisms Section, Bethesda, MD, USA; **Massachusetts General Hospital, Department of Medicine, Boston, MA, USA

Abstract

Ovarian cancer is a leading cause of cancer mortality in women. The aim of this study was to elucidate whether whey acidic protein (WAP) genes on chromosome 20q13.12, a region frequently amplified in this cancer, are expressed in serous carcinoma, the most common form of the disease. Herein, we report that a trio of WAP genes (*HE4*, *SLPI*, and *Elafin*) is overexpressed and secreted by serous ovarian carcinomas. To our knowledge, this is the first report linking Elafin to ovarian cancer. Fluorescence *in situ* hybridization analysis of primary tumors demonstrates genomic gains of the Elafin locus in a majority of cases. In addition, a combination of peptidomimetics, RNA interference, and chromatin immunoprecipitation experiments shows that Elafin expression can be transcriptionally upregulated by inflammatory cytokines through activation of the nuclear factor κB pathway. Importantly, using a clinically annotated tissue microarray composed of late-stage, high-grade serous ovarian carcinomas, we show that Elafin expression correlates with poor overall survival. These results, combined with our observation that Elafin is secreted by ovarian tumors and is minimally expressed in normal tissues, suggest that Elafin may serve as a determinant of poor survival in this disease.

Introduction

Ovarian cancer is a major cause of cancer-related mortality in women worldwide [1,2]. Fortuitous detection of early-stage organ-confined disease is associated with an excellent prognosis and a 5-year survival rate greater than 90% [3]. However, because of a lack of effective screening methods, conditions of most patients are diagnosed at an advanced stage when the opportunity for a surgical cure is drastically reduced. Furthermore, whereas most patients with advanced disease initially respond to standard chemotherapeutic regimens, the majority ultimately relapses with chemoresistant disease [3]. Therefore, there is a pressing need to develop new methods for early detection and prognostication. CA125 is an ovarian cancer serum biomarker clinically approved for monitoring response to treatment and detection of disease recurrence after definitive therapy [4]. However, its potential role in the early detection of ovarian cancer is controversial, in part because randomized screening trials of asymptomatic women with ovarian cancer mortality as an end point have yet to be completed [5].

Previous studies using comparative genomic hybridization and *in silico* chromosomal clustering reported that human chromosome 20q12-13.2 is consistently amplified in ovarian carcinomas and harbors genes that may play causal roles in the pathogenesis of the disease [6–10]. This region contains a cluster of 14 genes with homology to whey acidic protein (WAP) [11,12]. Among these genes is *HE4* [11]. On the basis of studies from our laboratory and others showing that HE4 is secreted by ovarian carcinomas and circulates in the blood stream of patients with the disease [13,14], we investigated whether other members of the WAP gene cluster are also overexpressed in this setting. Herein, we report that a trio of WAP genes, composed of *HE4*, *SLPI*, and *Elafin*, is overexpressed and secreted by ovarian carcinomas. Of the three, *Elafin* is the only one not previously reported to be associated with ovarian cancer [13–18]. Elafin is a serine proteinase inhibitor involved in inflammation and wound healing [19]. Our studies show that Elafin overexpression is associated with poor overall survival and is due, in part, to gains of the genomic locus and the ability to activate the nuclear factor κB (NF-κB) pathway in ovarian cancer cells.

Materials and Methods

Cell Lines

Twenty established cell lines were used to evaluate the messenger RNA and protein expression of the WAP genes. They included OVCA420, OVCA429, OVCAR-3, OV-90, SKOV3, CaOV3, OVCAR-5, OVCAR-8, IGROV1, TOV112D, TOV21G, ES2, HEYA8, MCF7, T47D, HCT116, HCT115, U2OS, 293, and IMR90. A majority of the lines were obtained from American Type Culture Collection (ATCC, Manassas, VA) and propagated in RPMI 1640 (Invitrogen, Carlsbad, CA) supplemented with 10% fetal bovine serum (FBS) and 1% penicillin/streptomycin (Invitrogen) at 37°C in a 5% CO_2-containing atmosphere. Two cell lines, OV-90 and OVCAR-3, were propagated in 1:1 MCDB105 and Media 199 (Sigma-Aldrich, St Louis, MO) with 15% FBS, whereas CaOV3, ES2, IGROV1, HCT116, HCT115, 293, MCF7, and IMR90 were propagated in Dulbecco's modification of Eagle medium (Cellgro, Herndon, VA) with 10% FBS. Expression of the different WAP genes, including *Elafin*, in these lines was compared with that of telomerase-immortalized ovarian surface epithelial (IOSE) as previously described [13]. The term human ovarian surface epithelium (HOSE) is used inter-changeably with IOSE.

Reverse Transcription–Polymerase Chain Reaction and Quantitative Polymerase Chain Reaction

RNA was purified as previously described [8]. Complementary DNA (cDNA) was synthesized from each cell line using 1 mg of RNA, extracted from the cell lines described above, using the iScript cDNA synthesis Kit (Bio-Rad, Hercules, CA) following the manufacturer's recommendations. Epididymis cDNA was synthesized from RNA obtained from BD Biosciences, Clontech (Palo Alto, CA). Polymerase chain reaction (PCR) primers are listed in Table W1. PCR products were identified on a 2.5% Tris-acctate-EDTA agarose gel. Quantitative amplification data were generated from 10 ng of cDNA on Bio-Rad's iCycler in conjunction with IQ SYBR Green (Bio-Rad, Hercules, CA). However, when confirming Elafin expression in microdissected late-stage high-grade serous tumors ($n = 20$) and normal OSE ($n = 10$), 50 ng of amplified RNA was used.

Recombinant Protein and Antibody Production

The full-length Elafin transcript was ligated into the pGEX-2T vector (GE Healthcare Bio-Sciences Corp, Piscataway, NJ). The modified vector was transformed into *Escherichia coli* Top10 (Invitrogen) where it was amplified. The insert-containing vector was sequenced to confirm positive selection. Induction and purification of recombinant protein were done as previously described [13]. Elafin-specific antibodies were raised by immunizing New Zealand White rabbits with glutathione *S*-transferase (GST) fusion protein composed of full-length Elafin and GST. Affinity-purified antibodies were generated as previously described [13]. Elafin monoclonal antibodies were purchased from Cell Sciences (Canton, MA). Recombinant untagged Elafin was purchased from R&D Systems (Minneapolis, MN).

Affymetrix GeneChip Amplification, Hybridization, and Image Acquisition

Total RNA quality for each tumor and normal OSE specimen was checked by BioAnalyzer (Agilent, Palo Alto, CA) before further manipulation. Two rounds of amplification were completed according to the Affymetrix Two-Cycle Amplification protocol using 25 ng of total RNA for tumor and normal OSE as previously described [20]. A 15-μg aliquot of amplified biotinylated RNA was hybridized to a Human U133 Plus 2.0 GeneChip array (Affymetrix, Santa Clara, CA). Arrays were scanned using the laser confocal GeneChip Scanner 3000 (Affymetrix).

Microarray Analysis

The Robust Multichip Analysis (RMA) algorithm was applied to the normal OSE and tumor array data. Biometric Research Branch (BRB) ArrayTools version 3.2.2 software developed by Dr. Richard Simon and Amy Peng Lam of the Biometrics Research Branch of the National Cancer Institute was used to filter and complete the statistical analysis. Only those probe sets present in greater than 50% of the arrays and displaying a variance in the top 50th percentile were evaluated.

Differentially expressed genes were identified for tumor and OSE specimens using a multivariate permutation *t*-test ($P < .05$). A total of 2000 permutations were completed to identify a list of probe sets containing fewer than 5% false-positives at a confidence of 90%. A random-variance model was selected to permit information sharing among probe sets.

Immunoblot Analysis

Western blots were done as previously described [13]. All blots were developed using HRP Oxidizing and Luminol Solutions (Boston Bioproducts, Worcester, MA) and analyzed on the FlourChem HD2 imaging system (Alpha Innotech, San Leandro, CA).

RNA Interference

Knockdown of NF-κB activity was achieved by targeting the p65 subunit with an small interfering RNA (siRNA) SMARTpool containing four individual siRNA against p65 (Upstate/Millipore, Charlottesville, VA). The SMARTpool sequences are 5′-GAUGAGAUCUUCCU-ACUGU, 5′-GGAUUGAGGAGAAACGUAA, 5′-CUCAAGAU-CUGCCGAGUGA, and 5′-GGCUAUAACUCGCCUAGUG and are collectively labeled as siRNA p65(1). A second independent siRNA against p65 (5′-GCUGAAGUGCAUCCAAAGGTT) was used as a control for off-target effects (Cell Signaling, Danvers, MA) and was labeled as siRNA p65(2). An NF-κB p65-specific antibody (sc-372; Santa Cruz Technologies, Santa Cruz, CA) was used to analyze total cell extracts from cells treated with the p65 SMARTpool *versus* control siRNA. Equal protein loading was confirmed by immunostaining of glyceraldehyde-3-phosphate dehydrogenase (Abcam, Cambridge, MA).

Tumor-Normal Northern Blot Analysis

Membranes loaded with RNA from matched tumor and normal tissue samples were purchased from Clontech (Cancer Profiling Arrays I and II; Mountain View, CA). An Elafin-specific probe was generated by random priming of Elafin cDNA using TaKaRa Ladderman Labeling Kit (Takara Bio, Inc, Madison, WI) according to the manufacturer's instructions. Hybridization of the membranes was carried out as described in the Cancer Profiling Array manual. The labeled membranes were placed in a phosphor screen cassette for 14 days before it was scanned on a Molecular Dynamics' STORM860 system (GE Healthcare Bio-Sciences Corp). The phosphoimage was analyzed using ImageQuant v1.2 (Molecular Dynamics; GE Healthcare Bio-Sciences Corp).

Chromatin Immunoprecipitation

The nucleotide sequence located 1 kb upstream of the start codon of Elafin was analyzed using a combination of algorithms that can predict potential transcription factor binding sites (TESS http://www.cbil. upenn.edu/cgi-bin/tess/tess and AliBaba http://darwin.nmsu.edu/ ~molb470/fall2003/Projects/solorz/aliBaba_2_1.htm) and previously published data [21,22]. We identified three potential NF-κB binding sites. TOV21G and OVCAR8 cells were cultured to approximately 70% confluence before the medium was changed to serum-free medium. Half of the plates were treated with 5 ng/ml of interleukin 1β (IL-1β) for 2 hours. The chromatin immunoprecipitation (ChIP) assay was done as previously described [23]. Briefly, we cross-linked cells using formaldehyde (1%) for 10 minutes at 37°C. The cells were washed and lysed before they were sonicated (Misonix Sonicator 3000; Misonix, Inc, Farmingdale, NY) three times for 10 seconds at maximum output to shear the DNA. DNA fragment size was confirmed at 0.5 to 1.0 kb by electrophoresis. Chromatin DNA was collected by centrifugation and an input sample was collected and stored in –80°C. Supernatant was diluted 1:10 in 1% Triton X-100, 2 mM EDTA, 150 mM NaCl, 20 mM Tris-HCl, pH 8.1 and incubated with either 1 μg of p65 antibody or 1 μg of anti–Golgi antibody (58K9; Abcam) and protein A beads overnight at 4°C. The beads were then washed six times in radio-immunoprecipitation buffer (Boston Bioproducts) and two times in

Tris-EDTA buffer before the samples were de–cross-linked in 1% SDS, 0.1 M NaHCO₃ at 65°C for 14 hours. De–cross-linked samples were purified using Qiagen's spin columns according to manufacturer's instructions (Qiagen, Valencia, CA). PCR (at 95°C for 5 minutes followed by 35 cycles at 95°C for 30 seconds, at 60°C for 30 seconds, at 72°C for 30 seconds, followed by 72°C for 5 minutes) was performed on (2 μg of total DNA) samples collected before IP(input) as well as after p65-specific and control immunoprecipitation. Primers were designed to span each of the putative NF-κB binding sites as well as two control regions located 2 kb upstream and 2 kb downstream of the Elafin transcription start site. Primer sequences are reported in Table W2.

Tissue Samples and Immunohistochemistry

After institutional review board approval, sections of formalin-fixed, paraffin-embedded (FFPE) human epididymis were obtained from the Department of Pathology at the Brigham and Women's Hospital (Boston, MA) to evaluate the expression of Elafin in this tissue and for subsequent use as positive control tissue. Elafin expression in normal human tissues was analyzed by immunohistochemistry (IHC) as previously described using a collection of normal human tissue blocks [13], whereas expression in ovarian and non–ovarian tumors was analyzed using high-density tissue microarrays (TMAs) made in-house (see below) or purchased from Biomax US (Rockville, MD). The Elafin affinity–purified rabbit antibody was used at a dilution of 1:1500 with heat-induced epitope retrieval as previously described [13]. Negative controls included protein A–purified preimmune serum, anti-GST antibodies purified as a byproduct of Elafin antibody production, and anti-Elafin antibodies preincubated with recombinant GST-Elafin protein before IHC. None of these controls generated a positive signal in IHC. HE4 localization using affinity-purified antibodies was done as previously described [13]. Slides were counterstained with Mayer hematoxylin.

Primary Tumor Cells

With institutional review board approval, primary ovarian carcinoma cells (DF lines) were isolated directly from peritoneal paracentesis of patients with advanced-stage ovarian cancer at the time of initial cyto-reductive surgery. Red blood cells were lysed as previously described [24], and the samples were enriched for tumor cells either by using immunomagnetic beads coupled to EpCAM antibodies (Dynal/Invitrogen) or by filtration using a 40-μm nylon cell strainer (BD Falcon, San Jose, CA) to isolate tumor cell spheres. Both methods enriched for tumor cells but the yield with the cell strainer was significantly better than with the magnetic EpCAM beads. In all cases, the epithelial nature of the cells was confirmed by EpCAM and HE4 antibody immunostaining as well as reverse transcription–PCR (RT-PCR) detection of CK7. For this study, we used only primary lines that were greater than 80% tumor pure after enrichment.

High-Density TMA

A TMA was constructed from 134 cases of high-grade late-stage ovarian papillary serous carcinoma who underwent primary cyto-reductive surgery at Brigham and Women's Hospital. Cases were identified by review of all pathology reports between January 1, 1999, and December 31, 2005, in the Brigham and Women's Hospital database that included a diagnosis of "ovarian cancer." The rationale for limiting the enrollment date to the year 1999 is that is when taxol became the standard of care, and the cutoff year of 2005 was established to allow

adequate follow-up time. All cases that met the eligibility criteria of International Federation of Gynecology and Obstetrics (FIGO) stage III or IV high-grade papillary serous ovarian carcinoma, pathology blocks available for generation of a TMA, and age requirements for one of two cohorts (≤55 years or ≥65 years of age at diagnosis) were included in the TMA (62 cases were from women ≤55 years of age, and 72 cases were from women ≥65 years of age). Patients with known *BRCA* mutations or with a history of another malignancy (excepting nonmelanoma skin cancers or noninvasive endometrial cancers) in the previous 5 years were excluded. Hematoxylin and eosin slides were reviewed to confirm the original diagnosis and to identify the most appropriate area of tumor for further studies. Corresponding FFPE tissue from each case was used to construct four high-density TMAs: two TMAs containing samples from the younger cohort and two TMAs containing samples from the older cohort. Four cores of tissue were taken from each case, with each core 0.8 mm in diameter. Five-micrometer-thick, unstained sections of the TMAs, as well as 5-µm-thick, unstained "whole mount" sections from the formalin-fixed paraffin-embedded tissue, were used for immunohistochemical analysis, and the findings were correlated with clinical data (age, optimal *vs* suboptimal cytoreduction status, platinum sensitivity, and overall survival) abstracted from the patient's medical records. Optimal surgical cytoreduction was defined as residual tumor 1 cm or less in diameter, and the duration of overall survival was determined from the date of diagnosis to either death or censored by the date of last follow-up. All pathology specimens and clinical data were collected under the approval of the institutional review board.

Fluorescence In Situ Hybridization

Four-micrometer whole-mount sections of Elafin-positive high-grade papillary serous carcinoma were mounted on standard glass slides and baked at 60°C for at least 2 hours, then deparaffinized and digested using methods described previously [25]. The following DNA fosmid probes were cohybridized: G248P8772D4 and G248P82920B4 (SpectrumGreen), which map to 20q13.12, the latter clone includes the entire coding sequence of *PI3/Elafin*, and D20Z1 (SpectrumOrange), which maps to 20p11.1-q11.1. The D20Z1 probe was purchased from Abbott Molecular/Vysis, Inc (Des Plaines, IL). Both fosmid probes were obtained from CHORI (www.chori.org), direct-labeled using nick translation and precipitated using standard protocols, and cohybridized as a contig probe. Final (total) fosmid probe concentration was approximately 50 to 100 ng/µl. D20Z1 final probe concentration followed manufacturer's recommendations.

Tissue sections and probes were codenatured, hybridized at least 16 hours at 37°C in a darkened humid chamber, washed in 2× SSC at 70°C for 10 minutes, rinsed in room temperature 2× SSC, and counterstained with 4′,6-diamidino-2-phenylindole (Abbott Molecular/Vysis, Inc). Slides were imaged using an Olympus BX51 fluorescence microscope (Olympus, Center Valley, PA). Individual images were captured using an Applied Imaging system running CytoVision Genus version 3.9 (Applied Imaging, Grand Rapids, MI), and all aberrations detected by fluorescence *in situ* hybridization (FISH) were reviewed and confirmed by a cytogeneticist (A.L.).

NEMO-Binding Domain (NBD) Assay

Cells were cultured until they reached 60% confluence, after which the medium was changed to FBS-depleted. The cells were incubated with 25 µM NEMO-Binding Domain (NBD) peptide (Calbiochem/EMD Biosciences, San Diego, CA) or scrambled peptide (Calbiochem/EMD Biosciences) for 24 hours before the addition of 5 ng/ml of IL-1β. After treatment with IL-1β, the cells were cultured for an additional 2 hours before RNA was harvested, and Elafin expression was monitored by quantitative RT-PCR. Scrambled peptides as well as nontreated cells were used as negative control.

Statistical Analysis

Clinical cases of late-stage ovarian serous carcinoma were scored for Elafin expression according to the following scheme: 0 = no positive cells, +1 = 1% to 5% positive cells, +2 = 6% to 50% positive cells and +3 = more than 50% positive cells (Figure 4). Samples were also scored from 1 to 3 depending on the staining intensity. All scoring was blinded and performed by two independent pathologists (R.D. and M.S.H.). The statistical analysis was done by a third party (J.L.) with no preconception of potential outcome. Before analysis of any survival data, cases were divided into a high-Elafin expressor group (scores of +2 or +3) and a low Elafin expressor group (scores of 0 or +1). Kaplan-Meier curves were plotted for these two groups to assess overall survival, and the difference between the curves was evaluated using the log-rank test. An estimate of the hazard ratio (HR) was calculated with a Cox proportional hazards model. Statistical analysis was performed using SAS version 9.1 software (SAS, Cary, NC).

Results

Elafin, HE4, and SLPI Constitute a Trio of Overexpressed WAP Genes in Ovarian Cancer

A panel of six ovarian cancer cell lines was screened for expression of WAP genes by RT-PCR. We found three WAP genes, *Elafin*, *HE4*, and secretory leukocyte protease inhibitor (*SLPI*), variably expressed in the cancer lines. Relative to the IOSE line, *HE4* and *Elafin* were overexpressed only in the cancer lines. Conversely, *SLPI* was more broadly expressed across all cell lines and IOSE (Figure 1*A*), consistent with our previous observations [13]. Unlike *HE4* and *SLPI*, *Elafin* expression has not previously been reported in ovarian cancer. We therefore sought to investigate the expression of *Elafin* in primary tumors. We used Affymetrix U133 Plus 2 chips to compare the gene expression profiles of microdissected late-stage high-grade ovarian serous carcinomas (*n* = 66) to profiles from microdissected OSE (*n* = 10). *Elafin* expression was three-fold higher in the serous late-stage carcinomas, a statistically significant result (Figure 1*B*). *Elafin* was also significantly overexpressed in early-stage high-grade serous carcinomas (*n* = 11), low-grade serous carcinomas (*n* = 18), and high-grade endometrioid carcinomas (*n* = 18), although there were fewer cases in these cohorts (Figure 1*B*). To confirm the expression profiling results, we conducted quantitative real-time PCR on 20 microdissected late-stage high-grade serous carcinomas and 10 microdissected OSE. *Elafin* transcript levels were more than 70-fold higher in the serous carcinomas compared with microdissected OSE (Figure 1*C*). We also examined Elafin protein expression in primary human late-stage high-grade serous tumors by IHC and found high levels of expression compared with OSE (Figure 1*D*). The specificity of the Elafin antibody was tested by Western blot analysis (Figure W1) and IHC controls as described in the Materials and Methods. A panel of normal benign human tissues was also examined by IHC for Elafin expression (Table W1). Interestingly, in the epididymis, an organ devoted to sperm maturation and the native site of WAP gene expression [11,26,27], expression of Elafin was restricted to the p63- and cytokeratin 7–positive basal cells, whereas HE4 expression was restricted to the apical portion of luminal cells (Figure 2), suggesting that Elafin may exhibit distinct biologic properties when compared with HE4.
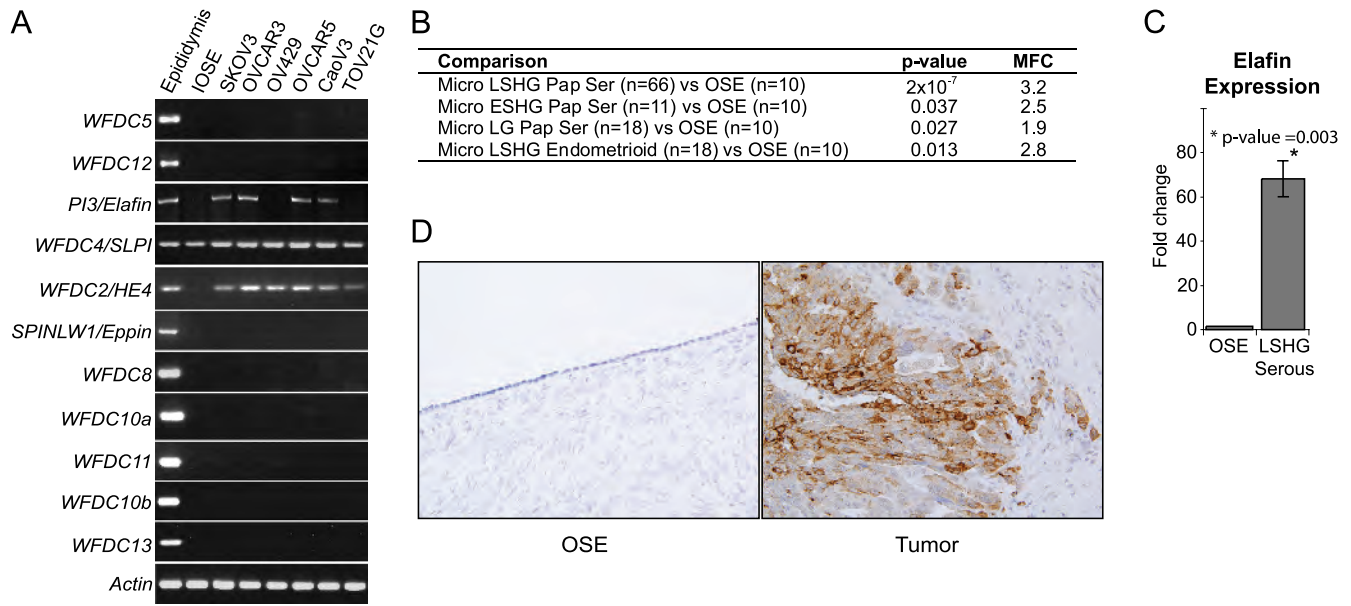
Figure 1. A trio of WAP genes is overexpressed in ovarian carcinomas. (A) Expression of the WAP genes was determined by semiquantitative RT-PCR. Epididymis served as a positive control for WAP expression, and telomerase IOSE served as a cell-of-origin control. *Elafin*, *SLPI*, and *HE4* are overexpressed in a panel of ovarian carcinomas. (B) Gene expression profiling of Elafin expression in different types of ovarian carcinomas and normal OSE. The tumors are divided into five groups: late-stage high-grade (LSHG) serous, early-stage high-grade (ESHG) serous, low-grade (LG) serous, and LSHG endometrioid. Elafin expression is significantly higher in all tumors compared with OSE. (C) Quantitative RT-PCR of *Elafin* expression in microdissected LSHG serous carcinomas ($n = 20$) compared with microdissected OSE ($n = 10$). LSHG serous cancers show a 70-fold increase of *Elafin* expression compared with OSE. (D) Expression of Elafin in OSE and serous carcinoma. Representative images from a panel of 8 normal ovaries and 20 late-stage high-grade serous carcinomas immunostained for Elafin. Original magnification, ×20.
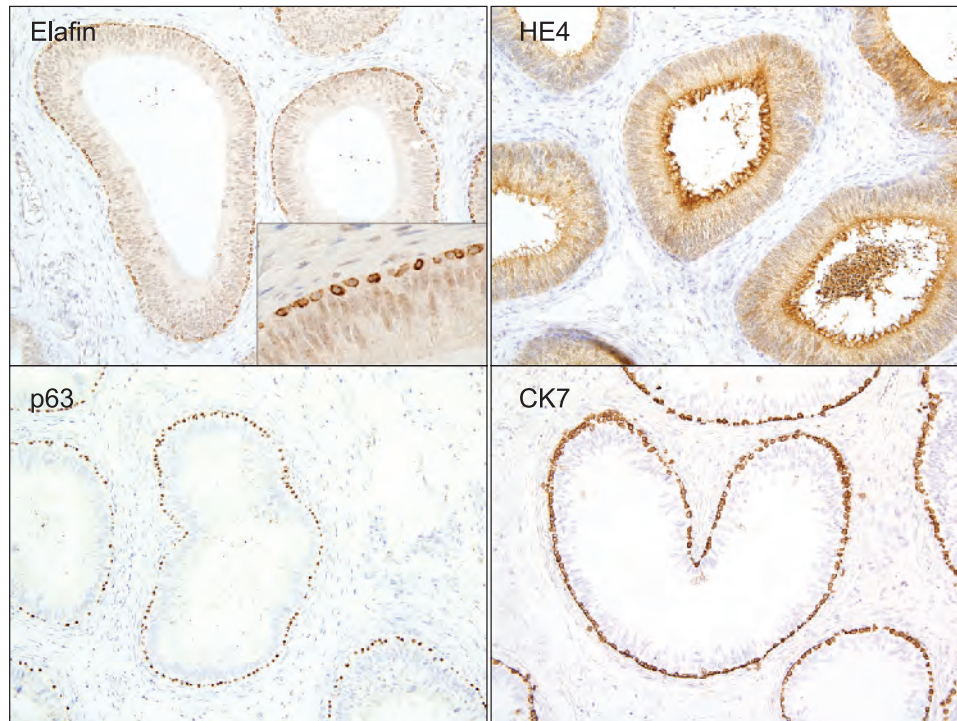

Figure 2. Expression of Elafin in human epididymis. IHC was performed on epididymis tissue using antibodies against Elafin, HE4, p63, and cytokeratin 7 (CK7). Elafin expression is limited to the p63- and CK7-positive basal cells, whereas HE4 is expressed in the luminal cell compartment.

Elafin Expression Is Restricted to Certain Tumor Types and Is Secreted by Primary Ovarian Carcinomas

Analysis of ovarian and non–ovarian cancer cell lines by RT-PCR revealed that *Elafin* expression is largely restricted to ovarian carcinoma lines, including OVCAR3, OVCAR5, and CaoV3 (Figure 3*A*). Consistent with previous reports [27], we did not observe *Elafin* expression in breast cancer cell lines (MCF7 and T47D). In addition, colon (HCT115, HCT116), osteosarcoma (U2OS), kidney (293), lung (Calu-1, NCI-H23), and brain (MO59K) cancer lines failed to express *Elafin* under these conditions (Figure 3*A* and data not shown). Normal diploid fibroblasts (IMR90 cells) were also negative for *Elafin* expression. The only non–ovarian cancer lines that expressed *Elafin* in this study were the bladder tumor line T24 and the cervical cancer line HeLa (data not shown). We also analyzed *Elafin* expression in tumors by hybridizing an Elafin cDNA probe to an ATLAS cancer array membrane (Clontech, Mountain View, CA), which was preloaded with matched RNA from normal/nonneoplastic tissue and tumor tissue derived from the same organ. Our results confirmed the higher expression of *Elafin* in ovarian tumors (T) *versus* matched normal (N) tissue (Figure 3*B*). The converse was true for breast normal-tumor pairs. Interestingly, we did observe robust *Elafin* expression in some non–ovarian tumors compared with the matched normal samples, including those from the lung, vulva, and skin, all with squamous histologic diagnosis (Figure 3*B*, *arrowheads*). Expression of *Elafin* by squamous cell carcinomas was previously reported [29–32], and we confirmed it by IHC using Elafin-specific antibodies on a TMA containing multiple tumors, including squamous cell carcinomas from various organ sites (Figure W2).

Elafin contains a signal peptide and is predicted to be a secreted protein [33]. Western blot analysis of conditioned medium from three ovarian cancer lines that express *Elafin* RNA revealed a secreted form of Elafin that comigrated with the recombinant protein at approximately 12 kDa (Figure 3*C*). In contrast, non–ovarian cancer lines did not secrete Elafin. We also isolated primary tumor cells directly from ascites fluid collected from eighteen patients with advanced serous carcinoma. Samples were enriched for tumor cells as described in the Materials and Methods, and the presence of tumor cells was confirmed by IHC with EpCAM and HE4 antibodies (data not shown). RT-PCR for *Elafin* showed that approximately half of the primary tumor samples express *Elafin*, and those that did also secreted Elafin (Figure 3, *D* and *E*; for example compare DF-03, -04, and -20 to DF-09, -22, and -30). As expected, the normal fibroblast line IMR90 was negative for both *Elafin* and *CK7* (Figure 3*D*).

Increased Elafin Expression in Ovarian Carcinomas Correlates with Poor Overall Survival

Our data indicate that Elafin is overexpressed and secreted by ovarian carcinomas. To determine whether Elafin expression is clinically significant, we immunostained an annotated TMA composed of 134 late-stage (FIGO stage III and IV) high-grade serous ovarian carcinomas with our rabbit polyclonal antibody against Elafin. Two pathologists (M.S.H. and R.D.) separately scored the sections in a blinded manner
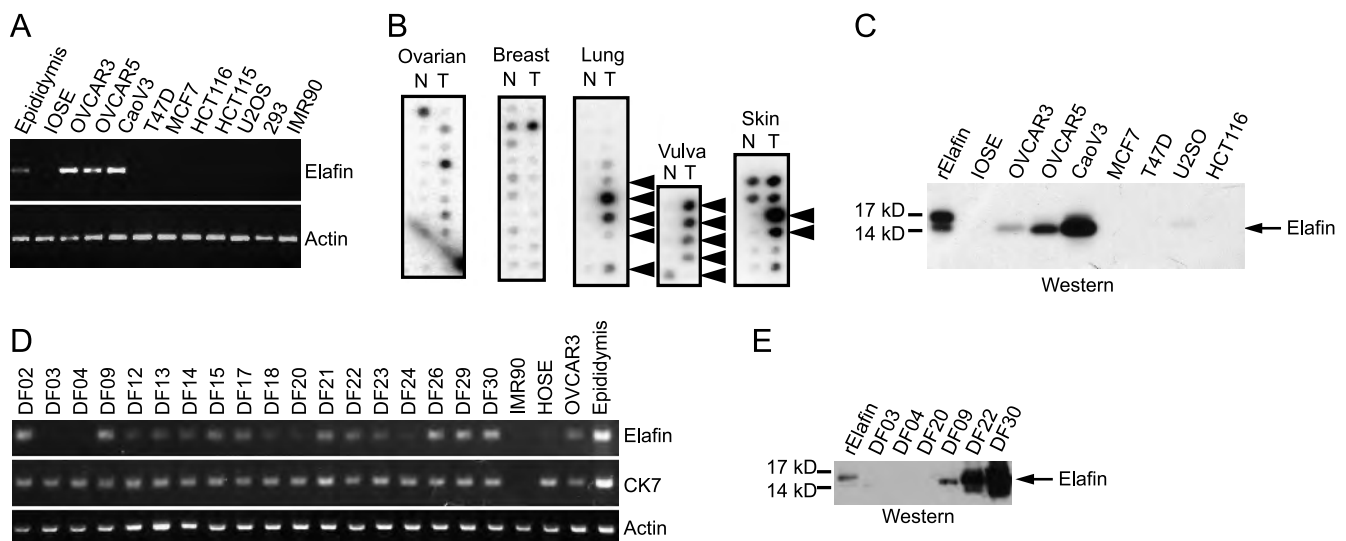

Figure 3. Elafin is uniquely expressed by ovarian and squamous cancers. (A) RT-PCR analysis shows that *Elafin* is specifically expressed in ovarian cancer cell lines (OVCAR3, OVCAR5, CaoV3), but not in other common epithelial cancer cell lines, including breast (T47D, MCF7), kidney (293), colon (HCT-116, HCT-115), and osteosarcoma (U2OS) or in normal diploid fibroblasts (IMR90). (B) Northern dot blot analysis for *Elafin* expression in matched tumor (T) and normal (N) tissue RNA. Higher *Elafin* expression is detected in ovarian tumor compared with normal tissue; the converse is found in breast. Other tumors that show an increase of *Elafin* expression were found to be squamous cell carcinomas (marked by black arrowheads). (C) Elafin is a secreted protein. Conditioned medium was collected from cell lines expressing *Elafin* RNA as well as nonexpressors. Recombinant Elafin served as a positive control. The two bands that are observed on the Western blot of the recombinant protein are due to a mixture of protein with or without a signal peptide. Elafin is detected in the conditioned medium collected from *Elafin*–RNA-expressing cells but not from nonexpressors. (D) Primary tumors express and secrete *Elafin*. *Elafin* expression was determined by semiquantitative RT-PCR (27 cycles) in a collection of enriched primary tumors (DF lines). *CK7* was used to validate the epithelial nature of the tumors. *Actin* served as a loading control. IMR90, HOSE, OVCAR3, and epididymis served as either negative or positive controls. (E) Primary tumors that express *Elafin* RNA also secreted it, as detected by Western blot analysis of conditioned medium collected from primary cell lines. The first three lanes are media from nonexpressing primary tumors and the last three are from high Elafin-expressing primary tumors. Recombinant Elafin is used as a positive control.
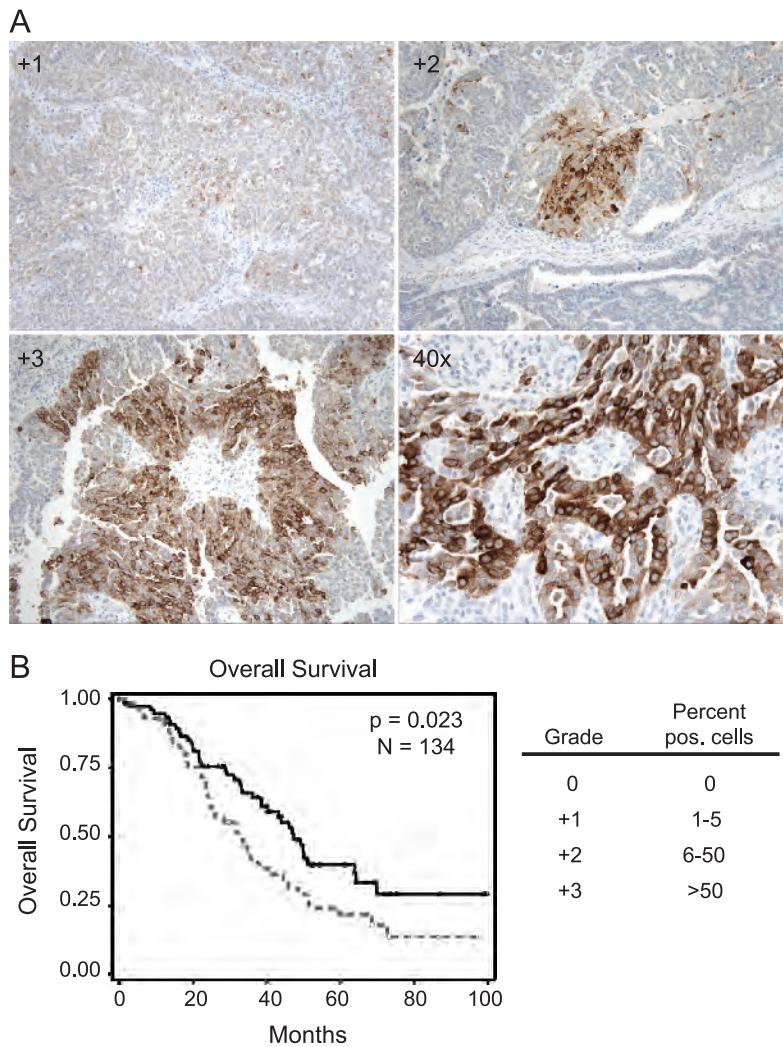
Figure 4. Elafin overexpression correlates with poor overall survival. IHC on 134 serous ovarian tumors (late-stage high-grade) with an Elafin antibody. (A) Examples of Elafin expression in ovarian tumors (10×). A few scattered positive cells (+1). Localized positive staining (+2). Large area of cells expressing Elafin (+3) and an example at a higher magnification (40×). (B) A Kaplan-Meier curve plotting overall survival of 77 patients with no or low Elafin expression (0 to +1, black) *versus* 57 high Elafin expression cases (+2 to +3, gray). Higher Elafin expression correlates with decreased survival ($P = .023$, $N = 134$) with a median survival of 47.3 months for patients with low Elafin expression *versus* 32.4 months for the patients that had tumors with higher Elafin expression. Scale used for scoring slides.

according to the grading scale from 0 to 3 (Figure 4). Clinical parameters included age, whether optimal cytoreduction had been achieved, platinum sensitivity, and overall survival. Unlike HE4, which tends to show diffuse expression in immunoreactive tumors [13], Elafin demonstrated a more focal staining pattern, ranging from scattered positive cells and clusters, to larger areas of positivity (Figure 4A). To reduce sampling error, whole-mount sections of all the cases were also stained for Elafin (Figure 4A). Seventy-seven cases exhibited no (score = 0) or low (score = 1) Elafin expression ($n = 33$: 0, $n = 44$: +1) and 57 exhibited high (score = 2 or 3) Elafin expression ($n = 45$: +2, $n = 12$: +3). Importantly, there were no statistical differences in the clinical characteristics of the two groups (Table 1). High Elafin expression in tumor tissue was associated with reduced survival in patients with primary ovarian cancer when the Cox univariate proportional hazards model

Table 1. Characteristics of High and Low Elafin Expressors.

	Elafin Low (0-1)	Elafin High (2-3)	$P*$
Mean age (years)	60.4	61.7	.60
Debulking			.17
Optimal	61/77 (79%)	40/57 (70%)	
Suboptimal	16/77 (21%)	15/57 (26%)	
Unknown	0/77 (0%)	2/57 (3.5%)	
Stage			.80
III	66/76 (87%)	48/57 (84%)	
IV	10/76 (13%)	9/57 (16%)	
Chemotherapy			.56
Platinum-based	64/77 (83%)	47/57 (82%)	
Nonplatinum	2/77 (2.6%)	0/57 (0%)	
Unknown	11/77 (14%)	10/57 (18%)	

*P value from Student's t-test for age; Fisher's exact test for all other variables.

Table 2. Multivariate Analysis.

	HR	95% CI	P
High elafin (2-3)	1.64	1.05-2.56	.03
Age	1.01	0.99-1.03	.23
Stage IV disease	1.37	0.72-2.60	.34
Optimal debulking	0.80	0.49-1.32	.39

was applied, with a HR for death of 1.65 for patients with high Elafin expression compared with low Elafin expression (95% confidence interval [CI], 1.07-2.54, P = .02). The relationship between Elafin expression levels and overall survival was visualized by a Kaplan-Meier plot (Figure 4B) and demonstrated a poorer survival in patients with high Elafin–expressing tumors (median survival, 32.4 months; 95% CI, 24.4-40.43 months) compared with those with no or low Elafin-expressing tumors (median survival, 47.3 months; 95% CI, 38.6-64.2 months). The P value for this difference was .02 by the log-rank test. Elafin remained significantly correlated with overall survival in a multivariate model incorporating age and debulking status (Table 2). Of note, although Elafin expression did not correlate with platinum sensitivity or resistance (defined as disease recurrence within 6 months of last receipt of platinum therapy; Table 1), 10 of 11 patients with primary platinum-refractory disease (defined as persistent disease or disease progression while receiving platinum-based therapy) had elevated Elafin expression. This correlation was highly statistically significant ($P = 8.4 \times 10^{-6}$).

Genomic Gains Drive Elafin Expression in Ovarian Cancers

The correlation between Elafin overexpression and patient outcome prompted us to examine the nature of its overexpression. As described

previously, the Elafin gene, *PI3*, is located on chromosome 20q13.12, a region frequently amplified in ovarian carcinomas [6–8]. We entertained the possibility that Elafin overexpression might be due to the amplification or gains of its genomic locus and designed DNA fosmid probes for FISH analysis. Whole-mount sections of 10 tumors that were scored +2 or +3 by IHC (Figure 4A) were evaluated by FISH for aberrations involving the *PI3* genomic locus (*green dots*). Chromosome 20 centromeric probes (red dots) served as controls for chromosomal copy number. All aberrations were verified by a cytogeneticist (A.H.L.). Copy number changes were classified as amplified when there was a ratio of test probe-control probe (T/C) of 3 or greater. T/C ratios of less than 3 but greater than 1 were interpreted as relative gains of *PI3*. T/C ratios of 1, even with greater than 2 copies of each probe were classified as polysomy. Although none of the tumors analyzed revealed amplification at the *PI3* locus, half of the samples showed gains at this locus relative to the centromeric probe (Figure 5, A and B). In addition, trisomy was observed in three of the remaining samples (Figure 5C) and disomy in two (Figure 5D). These data suggest that in a majority of Elafin-expressing tumors, the underlying mechanism of overexpression may be gains of the *PI3* locus and polysomy.

NF-κB Drives Expression of Elafin in Response to Inflammatory Mediators

Although gains at the *PI3* locus seem to be common in the tumors we evaluated, it was not the case for all Elafin-expressing tumors and it is likely that other regulatory mechanisms contribute to Elafin expression. Previous studies have demonstrated that Elafin expression is typically induced by inflammation at the transcriptional level; the most striking examples include psoriatic skin and inflammatory airway
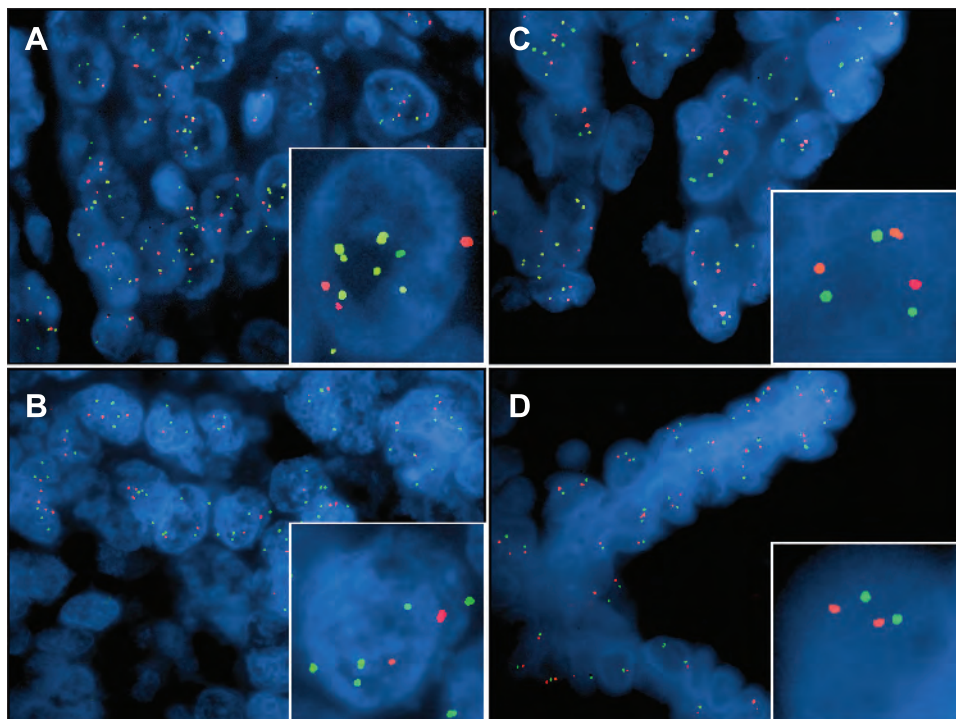

Figure 5. Genomic gains at the *PI3* locus underlie Elafin overexpression in ovarian carcinomas. FISH for the *PI3* locus. The G248P8772D4/G248P82920B4 fosmid probe (green) for *PI3* was cohybridized with the control chromosome 20 centromeric probe D20Z1 (red) on tissue sections of ten ovarian carcinomas that express high levels of Elafin protein by IHC. (A, B) Representative examples of gains of the *PI3* locus compared with the control probe. (C) Example of chromosome 20 trisomy. There are three foci of both the *PI3* probe and the centromere probe. (D) Example of disomy at both the *PI3* and centromeric loci.

disease [19,34]. Given the link between chronic inflammation and ovarian cancer pathogenesis [35–37], we examined whether inflammation might contribute to Elafin expression in ovarian cancer. A panel of 13 established ovarian cancer cell lines was screened by RT-PCR. Seven lines were found to strongly express *Elafin*, whereas six demonstrated

minimal or no expression of *Elafin* (Figure W3). Using both computer algorithms designed to predict transcription factor binding sites in promoter regions and previously published data (reviewed in Chowdhury et al. [22]), we identified three putative NF-κB transcription factor–binding sites in the promoter region of *Elafin* (Figure 6*A*). We then
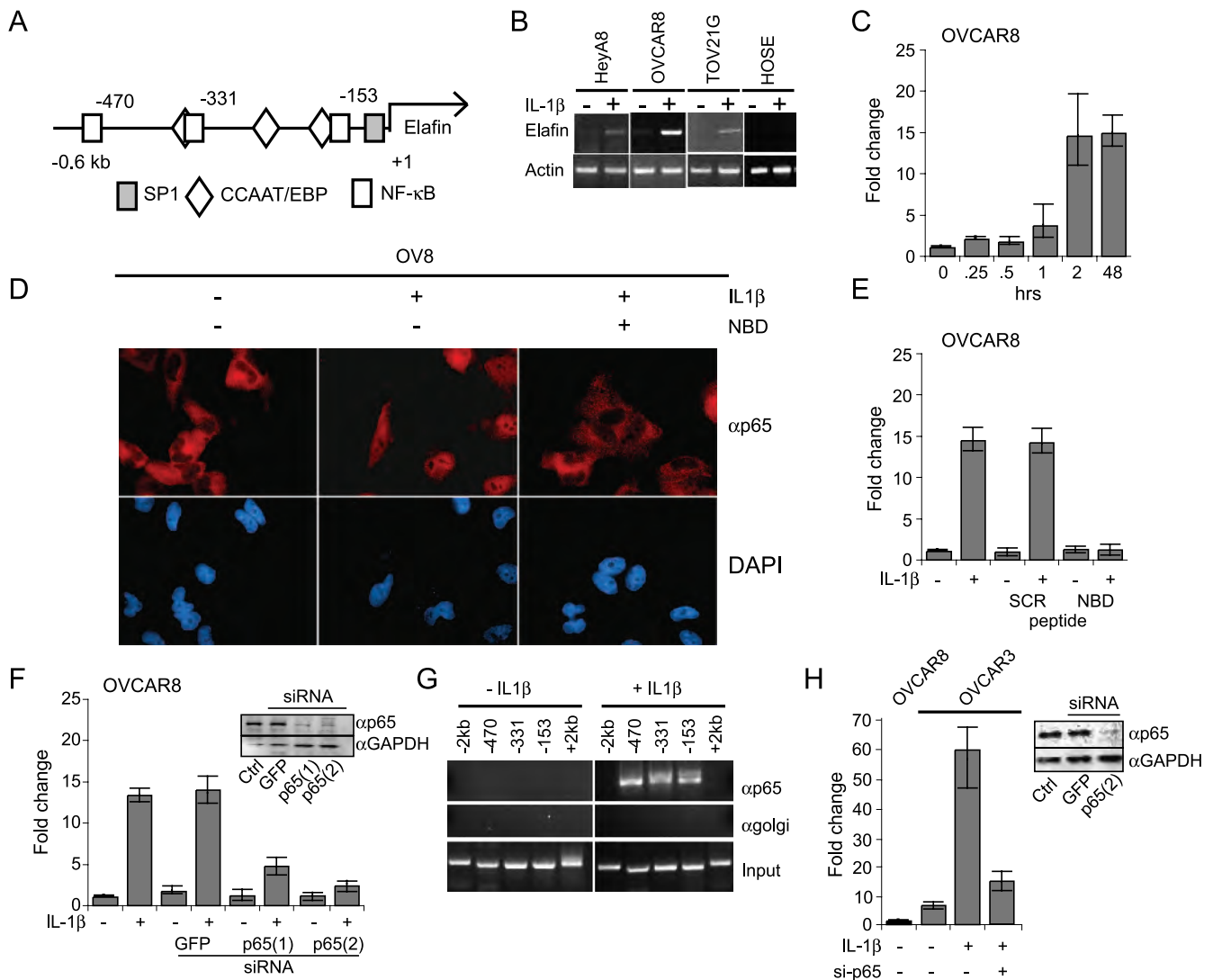

Figure 6. NF-κB drives the expression of *Elafin* in response to inflammatory mediators. (A) Schematic representation of predicted transcription factor binding sites in the *Elafin* promoter. The location of these sites relative to the first base of the start codon for *Elafin* (+1) is indicated by the number above the square. (B) A semiquantitative RT-PCR before and after IL-1β stimulation of no- or low-*Elafin* expressors. Cells were treated with 5 ng/ml IL-1β for 48 hours before RNA was harvested. An increase of *Elafin* expression was detected in HeyA8, OVCAR8, and TOV21G cells but not in HOSE. *Actin* serves as a loading control. (C) Time course of *Elafin* expression after cytokine treatment. OVCAR8 cells were treated with IL-1β, and *Elafin* expression was monitored by quantitative RT-PCR for 48 hours. (D) Immunofluorescent localization of p65. The NF-κB subunit p65 is normally localized in the cytoplasm of OVCAR8 cells (left panel) but is translocated into the nucleus upon cytokine stimulation using IL-1β (middle panel). The translocation of p65 is inhibited by blocking the NF-κB pathway with a peptide that specifically binds to the NBD, thus sequestering p65 to the cytoplasm (right panel). (E) Elafin induction by IL-1β can be abrogated by NBD. Scramble peptide does not inhibit the induction by IL-1β. (F) OVCAR8 cells transfected with siRNA against NF-κB subunit p65 72 hours before IL-1β treatment. Transfected cells show almost no increase in *Elafin* expression compared with nontransfected or cells transfected with siRNA against GFP. Two unique siRNA give rise to similar results. Inlayed panel shows efficiency of siRNA knockdown for p65 by Western blot; GAPDH serves as a loading control (right graph). (G) Occupancy of NF-κB sites on *Elafin* promoter by ChIP. In OVCAR8 cells, NF-κB (p65) binds to the predicted binding sites 2 hours after IL-1β treatment. Anti-Golgi antibodies were used as negative controls for the IP. Primers located 5′ and 3′ of the NF-κB sites (−2 and +2 kb, respectively) served as controls and yielded no product. Input DNA shows that all primers give rise to products on genomic DNA. (H) IL-1β can act through NF-κB to induce further Elafin expression in ovarian cancer lines that constitutively express *Elafin*. OVCAR-3 cells constitutively express *Elafin* compared with OVCAR-8 cell (Figure W3). Stimulation of OVCAR-3 cells with IL-1β increases Elafin expression even further. Knockdown of NF-κB activity with siRNA against the p65 subunit (Western blot, inset) abrogates the stimulus-induced increase but not the baseline levels of *Elafin* expression.

treated the ovarian cancer cells that normally express minimal or no *Elafin* (Figure W3) with the cytokine IL-1β, which is known to induce NF-κB recruitment to promoter elements of responsive genes [38]. Stimulation of HeyA8, OVCAR8, and TOV21G cells with IL-1β for 2 hours resulted in a marked expression of *Elafin* (Figure 6*B*). Tumor necrosis factor α, another proinflammatory cytokine, had a similar albeit weaker effect (data not shown). Importantly, under the same conditions, IL-1β did not induce the expression of *Elafin* in a HOSE line (Figure 6*B*). To determine the kinetics of *Elafin* induction, two cell lines, OVCAR8 and TOV21G, which normally express very low levels of *Elafin*, were treated with IL-1β, and *Elafin* expression was monitored over time. Two hours after IL-1β stimulation, a dramatic increase in *Elafin* expression was detected: 15-fold in OVCAR8 cells (Figure 6*C*) and 5-fold in TOV21G cells (data not shown). The increased expression lasted for more than 48 hours. In contrast, analysis of HE4 expression under the same conditions failed to demonstrate a similar effect (data not shown), suggesting that *Elafin* and *HE4* expressions are differentially regulated. The effect of IL-1β on Elafin levels in cells that normally do not express *Elafin* suggests that the NF-κB pathway may participate in driving *Elafin* expression. To test this hypothesis, we treated OVCAR8 cells with NEMO-binding domain (NBD) peptide, an IκB kinase (IKKγ) inhibitor [39], 24 hours before induction with IL-1β. IKKγ normally phosphorylates IκB and leads to its dissociation from the NF-κB complex, thus permitting nuclear entry and activation of NF-κB. Treatment of OVCAR8 cells with IL-1β results in the nuclear translocation of NF-κB, as measured by immunofluorescence for the p65 DNA binding subunit of NF-κB (Figure 6*D*), whereas NBD completely blocks the nuclear translocation of p65 in the presence of IL-1β (Figure 6*D*). Under these conditions, cells treated with 25 μM of the NBD inhibitor peptide before stimulation with IL-1β showed no increase in *Elafin* expression, whereas the scrambled peptide did not inhibit *Elafin* induction by IL-1β (Figure 6*E*). The effect of NBD was concentration-dependent (data not shown).

We further explored the potential direct involvement of NF-κB in the induction of *Elafin* expression using siRNA to deplete the levels of p65 before IL-1β treatment. Knockdown of p65 was confirmed by Western blot analysis using two different siRNA reagents (Figure 6*F, inset*). OVCAR8 cells treated with control siRNA (GFP) showed comparable levels of *Elafin* expression to those cells treated with IL-1β only. However, OVCAR8 cells that had been treated with siRNA against p65 showed greatly diminished induction of *Elafin* in response to IL-1β (Figure 6*F*). This is not likely due to an off-target effect of RNA interference (RNAi) because two different siRNA sequences gave a similar result. Finally, ChIP was used to address whether endogenous p65 occupies its cognate DNA binding sites on the *Elafin* promoter after cytokine induction, which would suggest that NF-κB directly drives *Elafin* expression. In both OVCAR8 (Figure 6*G*) and TOV21G cells (data not shown), there was no occupancy of the *Elafin* promoter by p65 in the absence of IL-1β. However, 2 hours after IL-1β treatment, all three binding sites were occupied (Figure 6*G*). This binding is specific for three reasons: 1) it is only observed in response to a stimulus (IL-1β), 2) control antibodies (α-Golgi) do not precipitate binding activity, and 3) binding is specific to the NF-κB sites because binding was not seen at sequence upstream and downstream of the NF-κB consensus sites (Figure 6*G*). Because the genomic resolution of ChIP is limited by the size of DNA fragments generated (typically 500 bp after sonication), it cannot be concluded that all three NF-κB sites are occupied simultaneously because they all exist within approximately 300 bp of one another (Figure 6*A*). Nonetheless, the results demonstrate that

p65 occupancy is dependent on cytokine stimulation. In addition, the overall results strongly argue that induction of *Elafin* expression by IL-1β is mediated by the NF-κB pathway in ovarian cancer cells that normally do not express the protein. Interestingly, it should be noted that treatment with IL-1β can also induce higher levels of *Elafin* expression in cell lines that constitutively express Elafin, such as OVCAR3 cells (Figures 6*H* and W3). In this setting, knocking down the p65 subunit of NF-κB resulted in a loss of the stimulus-induced expression of *Elafin*, but there was no effect on the baseline level of expression (data not shown). This latter effect is consistent with our observation that constitutive expression by ovarian tumors is likely mediated by genomic gains of the *PI3* locus (Figure 5).

Discussion

In this study, we demonstrate that Elafin is overexpressed and secreted by ovarian carcinomas. To our knowledge, this is the first report linking Elafin to ovarian cancer. We show that *Elafin* expression is regulated, in part, by gains of the genomic locus and polysomy. We also show that inflammatory mediators can induce expression through the NF-κB pathway, which plays a pivotal role in the link between inflammation and cancer [40]. We could specifically block the induction of *Elafin* expression with a compound (NBD peptide) that inhibits the proper assembly of the IKK complex necessary for activation of NF-κB. RNAi directed against the p65 DNA binding subunit of NF-κB in the presence or absence of IL-1β demonstrated that knockdown of this subunit abrogated the induction of Elafin expression in response to this inflammatory mediator. Finally, using chromatin immunoprecipitation experiments, we found that NF-κB can specifically occupy cognate binding sites in the *Elafin* promoter only after stimulation with cytokine. These findings are consistent with previous studies reporting a role for NF-κB in mediating Elafin expression in pulmonary epithelial cells in response to inflammatory mediators [34,41].

The role of Elafin in ovarian carcinoma is currently undefined. Elafin is a serine proteinase inhibitor [19]. Its expression, and that of SLPI, is induced under conditions of inflammation and wound healing [42]. Studies on *SLPI* knockout mice show impaired cutaneous wound healing with increased inflammation and elastase proteinase activity [43]. Whether Elafin plays a similar role is difficult to ascertain because there is no direct homolog of Elafin in mouse [44]. Moreover, although SLPI and Elafin were initially discovered because of their antiproteinase activity, subsequent studies revealed diverse functions including antimicrobial properties and roles in regulating the innate immune system [19]. More recently, several studies showed that overexpression of SLPI is common in certain tumors including pancreatic, uterine, ovarian, and thyroid carcinomas (reviewed in Bouchard et al. [42]). One study in particular identified *SLPI* among four genes associated with metastasis and lymph node involvement in breast cancer [45] and another showed that high *SLPI* expression is associated with decreased disease-free survival and poor overall survival in breast cancer [46]. The function of SLPI and its antiproteinase activity in this setting are unclear. With regard to Elafin, a connection with cancer is beginning to emerge. A limited body of work shows that Elafin is expressed in a significant number of squamous cell carcinomas [29–32], a finding we have confirmed in this study. However, it is unclear whether its expression in these tumors is associated with clinical outcomes. A more recent study identified Elafin expression in glioblastoma multiforme and showed a correlation with poor outcome [47].

Our analysis of annotated TMAs and corresponding whole-mount tissue sections of ovarian high-grade late-stage serous carcinomas shows

that the high expression of Elafin is associated with a poorer overall survival compared with ovarian tumors that express no or low levels of Elafin. Whether Elafin is simply a surrogate for aggressive tumors or it actually functionally contributes to tumor behavior by an as yet undefined mechanism remains to be determined. However, if Elafin secretion leads to its circulation in the bloodstream, it is tempting to speculate that Elafin may serve as a surrogate for more aggressive, possibly more chemoresistant carcinomas that may benefit from alternative therapies. Consistent with this hypothesis, we found that platinum-refractory tumors in our clinical data set were very likely to have elevated levels of Elafin expression, a finding that warrants further investigation.

Acknowledgments

References

[1] Jemal A, Siegel R, Ward E, Hao Y, Xu J, Murray T, and Thun MJ (2008). Cancer statistics, 2008. *CA Cancer J Clin* **58**, 71–96.

[2] Stewart B and Kleihues P (2003). *WHO World Cancer Report.* Lyon, France: IARC Press.

[3] Cannistra SA (2004). Cancer of the ovary. *N Engl J Med* **351**, 2519–2529.

[4] Bast RC Jr (2003). Status of tumor markers in ovarian cancer screening. *J Clin Oncol* **21**, 200–205.

[5] Drapkin R, Clauss A, and Skates S (2008). Urokinase-type plasminogen activator receptor: a beacon of malignancy? *Clin Cancer Res* **14**, 5643–5645.

[6] Israeli O, Goldring-Aviram A, Rienstein S, Ben-Baruch G, Korach J, Goldman B, and Friedman E (2005). *In silico* chromosomal clustering of genes displaying altered expression patterns in ovarian cancer. *Cancer Genet Cytogenet* **160**, 35–42.

[7] Iwabuchi H, Sakamoto M, Sakunaga H, Ma YY, Carcangiu ML, Pinkel D, Yang-Feng TL, and Gray JW (1995). Genetic analysis of benign, low-grade, and high-grade ovarian tumors. *Cancer Res* **55**, 6172–6180.

[8] Kiechle M, Jacobsen A, Schwarz-Boeger U, Hedderich J, Pfisterer J, and Arnold N (2001). Comparative genomic hybridization detects genetic imbalances in primary ovarian carcinomas as correlated with grade of differentiation. *Cancer* **91**, 534–540.

[9] Sonoda G, Palazzo J, du Manoir S, Godwin AK, Feder M, Yakushiji M, and Testa JR (1997). Comparative genomic hybridization detects frequent overrepresentation of chromosomal material from 3q26, 8q24, and 20q13 in human ovarian carcinomas. *Genes Chromosomes Cancer* **20**, 320–328.

[10] Tanner MM, Grenman S, Koul A, Johannsson O, Meltzer P, Pejovic T, Borg A, and Isola JJ (2000). Frequent amplification of chromosomal region 20q12-q13 in ovarian cancer. *Clin Cancer Res* **6**, 1833–1839.

[11] Clauss A, Lilja H, and Lundwall A (2002). A locus on human chromosome 20 contains several genes expressing protease inhibitor domains with homology to whey acidic protein. *Biochem J* **368**, 233–242.

[12] Lundwall A and Clauss A (2002). Identification of a novel protease inhibitor gene that is highly expressed in the prostate. *Biochem Biophys Res Commun* **290**, 452–456.

[13] Drapkin R, von Horsten HH, Lin Y, Mok SC, Crum CP, Welch WR, and Hecht JL (2005). Human epididymis protein 4 (HE4) is a secreted glycoprotein that is overexpressed by serous and endometrioid ovarian carcinomas. *Cancer Res* **65**, 2162–2169.

[14] Hellstrom I, Raycraft J, Hayden-Ledbetter M, Ledbetter JA, Schummer M, McIntosh M, Drescher C, Urban N, and Hellstrom KE (2003). The HE4 (WFDC2) protein is a biomarker for ovarian carcinoma. *Cancer Res* **63**, 3695–3700.

[15] Devoogdt N, Revets H, Ghassabeh GH, and De Baetselier P (2004). Secretory leukocyte protease inhibitor in cancer development. *Ann N Y Acad Sci* **1028**, 380–389.

[16] Hough CD, Cho KR, Zonderman AB, Schwartz DR, and Morin PJ (2001). Coordinately up-regulated genes in ovarian cancer. *Cancer Res* **61**, 3869–3876.

[17] Simpkins FA, Devoogdt NM, Rasool N, Tchabo NE, Alejandro EU, Kamrava MM, and Kohn EC (2008). The alarm anti-protease, secretory leukocyte protease inhibitor, is a proliferation and survival factor for ovarian cancer cells. *Carcinogenesis* **29**, 466–472.

[18] Tsukishiro S, Suzumori N, Nishikawa H, Arakawa A, and Suzumori K (2005). Use of serum secretory leukocyte protease inhibitor levels in patients to improve specificity of ovarian cancer diagnosis. *Gynecol Oncol* **96**, 516–519.

[19] Williams SE, Brown TI, Roghanian A, and Sallenave JM (2006). SLPI and elafin: one glove, many fingers. *Clin Sci (Lond)* **110**, 21–35.

[20] Cuenca J and Bonome C (2005). Off-pump coronary artery bypass grafting and other minimally invasive techniques. *Rev Esp Cardiol* **58**, 1335–1348.

[21] Yokota T, Bui T, Liu Y, Yi M, Hunt KK, and Keyomarsi K (2007). Differential regulation of elafin in normal and tumor-derived mammary epithelial cells is mediated by CCAAT/enhancer binding protein beta. *Cancer Res* **67**, 11272–11283.

[22] Chowdhury MA, Kuivaniemi H, Romero R, Edwin S, Chaiworapongsa T, and Tromp G (2006). Identification of novel functional sequence variants in the gene for peptidase inhibitor 3. *BMC Med Genet* **7**, 49.

[23] Das PM, Ramachandran K, vanWert J, and Singal R (2004). Chromatin immuno-precipitation assay. *Biotechniques* **37**, 961–969.

[24] Barker SD, Casado E, Gomez-Navarro J, Xiang J, Arafat W, Mahasreshti P, Pustilnik TB, Hemminki A, Siegal GP, Alvarez RD, et al. (2001). An immunomagnetic-based method for the purification of ovarian cancer cells from patient-derived ascites. *Gynecol Oncol* **82**, 57–63.

[25] Firestein R, Bass AJ, Kim SY, Dunn IF, Silver SJ, Guney I, Freed E, Ligon AH, Vena N, Ogino S, et al. (2008). *CDK8* is a colorectal cancer oncogene that regulates beta-catenin activity. *Nature* **455**, 547–551.

[26] Kirchhoff C, Habben I, Ivell R, and Krull N (1991). A major human epididymis-specific cDNA encodes a protein with sequence homology to extracellular proteinase inhibitors. *Biol Reprod* **45**, 350–357.

[27] Lundwall A and Ulvsback M (1996). The gene of the protease inhibitor SKALP/elafin is a member of the REST gene family. *Biochem Biophys Res Commun* **221**, 323–327.

[28] Zhang M, Zou Z, Maass N, and Sager R (1995). Differential expression of elafin in human normal mammary epithelial cells and carcinomas is regulated at the transcriptional level. *Cancer Res* **55**, 2537–2541.

[29] Westin U, Nystrom M, Ljungcrantz I, Eriksson B, and Ohlsson K (2002). The presence of elafin, SLPI, IL1-RA and STNFα RI in head and neck squamous cell carcinomas and their relation to the degree of tumour differentiation. *Mediators Inflamm* **11**, 7–12.

[30] Yoshida N, Egami H, Yamashita J, Takai E, Tamori Y, Fujino N, Kitaoka M, Schalkwijk J, and Ogawa M (2002). Immunohistochemical expression of SKALP/elafin in squamous cell carcinoma of human lung. *Oncol Rep* **9**, 495–501.

[31] Alkemade HA, Molhuizen HO, van Vlijmen-Willems IM, van Haelst UJ, and Schalkwijk J (1993). Differential expression of SKALP/Elafin in human epidermal tumors. *Am J Pathol* **143**, 1679–1687.

[32] Yamamoto S, Egami H, Kurizaki T, Ohmachi H, Hayashi N, Okino T, Shibata Y, Schalkwijk J, and Ogawa M (1997). Immunohistochemical expression of SKALP/elafin in squamous cell carcinoma of the oesophagus. *Br J Cancer* **76**, 1081–1086.

[33] Wiedow O, Schroder JM, Gregory H, Young JA, and Christophers E (1990). Elafin: an elastase-specific inhibitor of human skin. Purification, characterization, and complete amino acid sequence. *J Biol Chem* **265**, 14791–14795.

[34] Bingle L, Tetley TD, and Bingle CD (2001). Cytokine-mediated induction of the human elafin gene in pulmonary epithelial cells is regulated by nuclear factor-κB. *Am J Respir Cell Mol Biol* **25**, 84–91.

[35] Ness RB and Cottreau C (1999). Possible role of ovarian epithelial inflammation in ovarian cancer. *J Natl Cancer Inst* **91**, 1459–1467.

[36] Ness RB, Grisso JA, Cottreau C, Klapper J, Vergona R, Wheeler JE, Morgan M, and Schlesselman JJ (2000). Factors related to inflammation of the ovarian epithelium and risk of ovarian cancer. *Epidemiology* **11**, 111–117.

[37] Wang X, Wang E, Kavanagh JJ, and Freedman RS (2005). Ovarian cancer, the coagulation pathway, and inflammation. *J Transl Med* **3**, 25.

[38] Hayden MS and Ghosh S (2008). Shared principles in NF-κB signaling. *Cell* **132**, 344–362.

[39] May MJ, Marienfeld RB, and Ghosh S (2002). Characterization of the Iκ B-kinase NEMO binding domain. *J Biol Chem* **277**, 45992–46000.

[40] Naugler WE and Karin M (2008). NF-κB and cancer-identifying targets and mechanisms. *Curr Opin Genet Dev* **18**, 19–26.

[41] Sallenave JM, Shulmann J, Crossley J, Jordana M, and Gauldie J (1994). Regulation of secretory leukocyte proteinase inhibitor (SLPI) and elastase-specific inhibitor (ESI/elafin) in human airway epithelial cells by cytokines and neutrophilic enzymes. *Am J Respir Cell Mol Biol* **11**, 733–741.
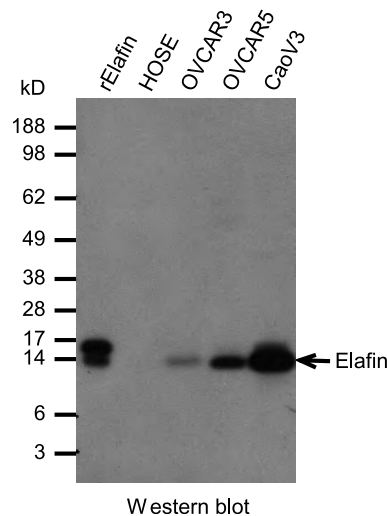
[42] Bouchard D, Morisset D, Bourbonnais Y, and Tremblay GM (2006). Proteins with whey-acidic-protein motifs and cancer. *Lancet Oncol* **7**, 167–174.

[43] Ashcroft GS, Lei K, Jin W, Longenecker G, Kulkarni AB, Greenwell-Wild T, Hale-Donze H, McGrady G, Song XY, and Wahl SM (2000). Secretory leukocyte protease inhibitor mediates non-redundant functions necessary for normal wound healing. *Nat Med* **6**, 1147–1153.

[44] Clauss A, Lilja H, and Lundwall A (2005). The evolution of a genetic locus encoding small serine proteinase inhibitors. *Biochem Biophys Res Commun* **333**, 383–389.

[45] Kluger HM, Chelouche Lev D, Kluger Y, McCarthy MM, Kiriakova G, Camp RL, Rimm DL, and Price JE (2005). Using a xenograft model of human breast cancer metastasis to find genes associated with clinically aggressive disease. *Cancer Res* **65**, 5578–5587.

[46] Cimino D, Fuso L, Sfiligoi C, Biglia N, Ponzone R, Maggiorotto F, Russo G, Cicatiello L, Weisz A, Taverna D, et al. (2008). Identification of new genes associated with breast cancer progression by gene expression analysis of predefined sets of neoplastic tissues. *Int J Cancer* **123**, 1327–1338.

[47] Saidi A, Javerzat S, Bellahcene A, De Vos J, Bello L, Castronovo V, Deprez M, Loiseau H, Bikfalvi A, and Hagedorn M (2008). Experimental anti-angiogenesis causes upregulation of genes associated with poor survival in glioblastoma. *Int J Cancer* **122**, 2187–2198.

Table W1. Elafin Protein Expression in Normal Human Tissues.

Normal Tissues		Positive/Tested	Histologic Description
Esophagus		2/2	Mature keratinocytes
Stomach		0/3	
Gallbladder		0/5	
Duodenum		0/6	
Colon		0/6	
Pancreas	Islet cells:	0/3	
	Glandular cells:	2/3	Weak in ductal epithelium
Liver	Hepatocytes:	0/5	Weak in bile ducts
Spleen		0/2	
Lymph node		0/3	
Lung		0/6	
Trachea	Epithelium:	2/5	Weak, focal
	Submucosal glands:	5/5	Moderate-to-strong
Tonsil		2/2	Squamous epithelium
Thyroid		0/6	
Heart muscle		0/2	
Kidney	Glomeruli:	0/9	
	Collecting tubules:	6/9	Weak-to-moderate
Brain		0/2	
Breast		7/9	Ductal epithelium
Ovary		0/8	
Fallopian tubes		1/6	Focal
Endometrium		0/4	
Cervix	Glandular cells:	0/3	
	Squamous epithelium:	6/6	
Epididymis		3/3	Only in basal cells
Prostate		0/6	

Table W2. Primer Used for PCRs.

			$5' \rightarrow 3'$
RT-PCR			
Elafin		Forward	GCTCTTAGCCAAACACCTTCCTGA
		Reversed	GGCCTTTGACAGTGTCTTGACCTT
		Forward	AGGTCCAGTCTCCACTAAGC
		Reversed	AGCCTTCACAGCACTTCTTG
Actin		Forward	ACAGAGCCTCGCCTTTGC
		Reversed	AGGATGCCTCTCTTGCTCTG
h36b4		Forward	ATCAACGGGTACAAACGAGTCCTG
		Reversed	AAGGCAGATGGATCAGCCAAGAAG
WFDC5		Forward	GGACCAACGGAAAGAGTTCA
		Reversed	GACTCCCAGGAGGAGAAACC
WFDC12		Forward	ACCTGGTGCTCCTCCCTAAT
		Reversed	TCTAGAGGCTGGGAAGTCCA
SLPI		Forward	AATGCCTGGATCCTGTTGAC
		Reversed	AAAGGACCTGGACCACACAG
WFDC2/HE4		Forward	CGGCTTCACCCTAGTCTCAG
		Reversed	CCTCCTTATCATTGGGCAGA
EPPIN		Forward	ACAAGAAGTGTTGTGTCTTCAGCTGCGG
		Reversed	TGGCAGCCACCATAGACAAACATGGAGC
WFDC8		Forward	GCTTTGGAGTGGACTTCTGC
		Reversed	TTCTTGAAAGGGATCCATGC
WFDC10a		Forward	ACAACCTGGCCAGACATAGG
		Reversed	TGCTTGACAATCTCGGTGAG
WFDC11		Forward	CGTCGAAACCAGTGGAGATT
		Reversed	TGTTTGCTGTTGTCCAGCTC
WFDC13		Forward	CCAGTTCCTGGTGGTGTTCT
		Reversed	TTGATTCTGTTGCGCTTTTG
ChIP			
–2 kb		Forward	TCTTTAGGAGTGCAATTGCTGA
		Reversed	ATTTTAGATTTGAATGGGTTGTTT
+2 kb		Forward	GATGTGAATGAGGAGGCAAGA
		Reversed	GAGTGGGTCAACAGGAGAGC
NF-κB –153		Forward	GGAAAACTCTTGGGACAATCA
		Reversed	CCTCATGGTGTCAGGAAGGT
NF-κB –331		Forward	GGAGAAACACTTGGTTTTGTAA
		Reversed	CAGAGTAGAAGTGCTGGCTCA
NF-κB –479		Forward	GAAAGGCCGTCTCTGAAACA
		Reversed	CAAACCCCACCCAGATCTAC

Figure W1. Elafin is secreted by ovarian cancer cell lines. Conditioned medium was harvested from cancer lines and HOSE as indicated. Equal protein was loaded on a 4% to 12% Bis-Tris polyacrylamide gel. After transfer, the blot was probed with affinity-purified rabbit poly antibodies against Elafin (1:1000 dilution).
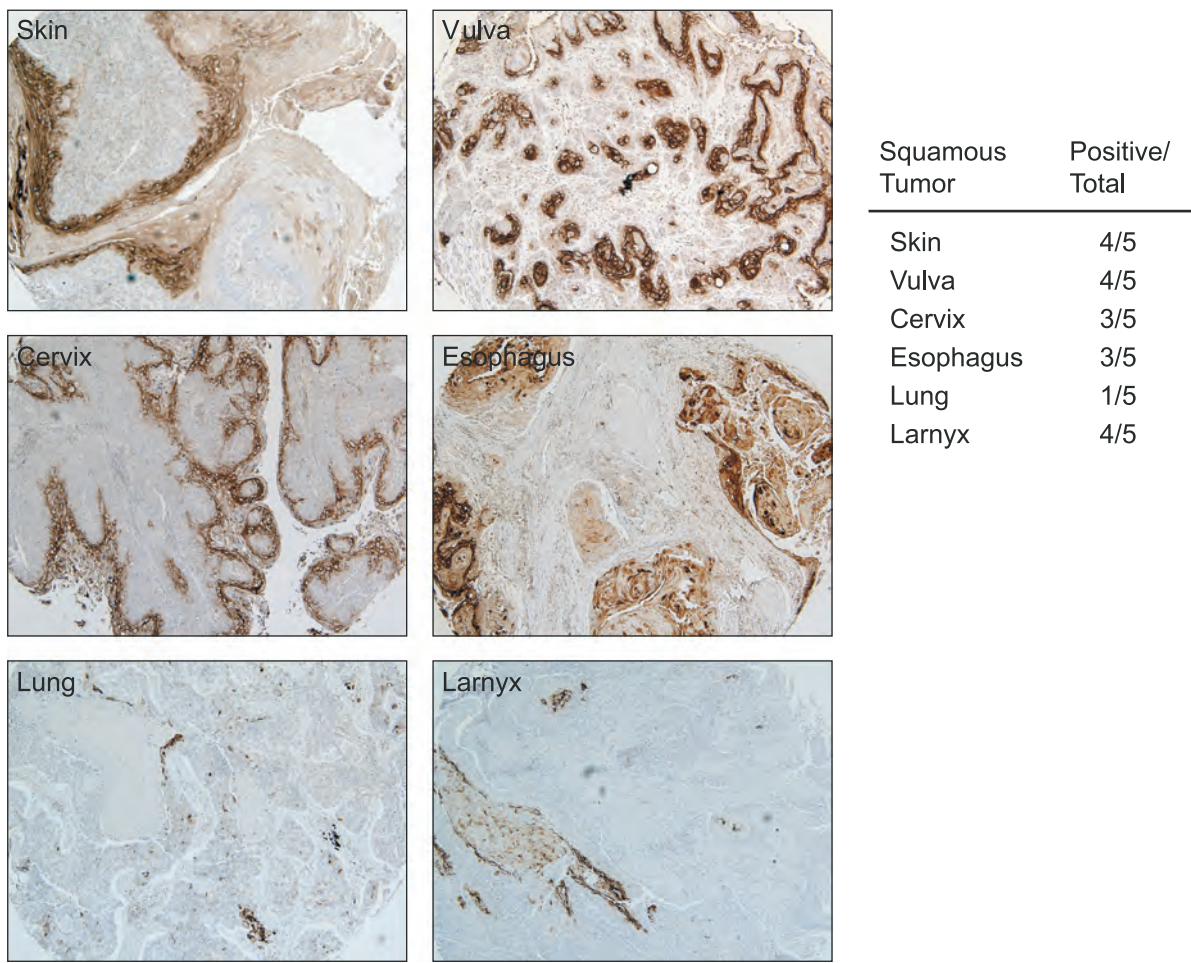
Squamous Tumor	Positive/ Total
Skin	4/5
Vulva	4/5
Cervix	3/5
Esophagus	3/5
Lung	1/5
Larnyx	4/5

Figure W2. Expression of Elafin in Squamous Carcinomas. A multiple-organ squamous cell carcinoma TMA (BC00019; Biomax US) was immunostained with affinity-purified antibodies against Elafin. Results are tabulated on the right.
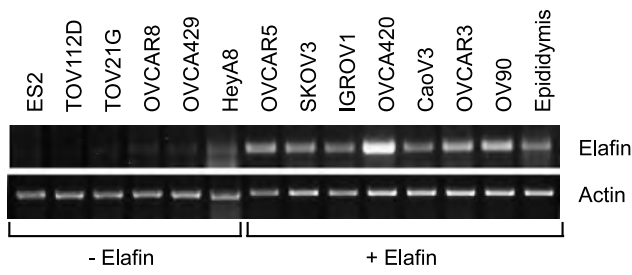

Figure W3. Elafin expression in a panel of 13 ovarian cancer cell lines. Elafin expression was determined by semiquantitative RT-PCR (27 cycles). Seven of the 13 lines were found to express Elafin. Actin served as a loading control.